날개짓 비행체의 양력 변위

Lift Force Variation of Flapping Wing

홍 영 선*
Young-Sun, Hong

ABSTRACT

Using the more common conventional chordwise aerodynamic approach, flapping a flat plate wing with zero degree chordwise pitch angle of attack and no relative wind should not produce lift. However, in hover, with no forward relative velocity and zero degree chordwise pitch angle of attack, flapping flat plate wings does in fact produce lift. In the experiments performed for this paper, the flapping motion is considered pure(downstroke and upstroke) with no flapping stroke plane inclination angle. No changes in chordwise pitch angle are made. The total force is measured using a force transducer and the net aerodynamic force is determined from this measured total force by subtracting the experimentally determined inertial contribution. These experiments were repeated at various flapping frequencies and for various wing planform sizes for flat plate wings. The trends in the aerodynamic lift variation found using a force transducer have nearly identical shape for various flapping frequencies and wing planform sizes.

주요기술용어(주제어) : Flapping Wing, Low Re, DPIV, Inertial Force

1. Introduction

Aerodynamicists have used the some theories to explain how airfoils generate lift. The principle of equal transit times is often mistakenly asserted as the manner in which a wing generates lift. This principle states that the pressure over the top of the airfoil creates a region of pressure lower than the bottom of an airfoil because flow over the curved upper surface would have to have greater velocity than that at the lower surface which is more flat. In reality, the principle of equal transit times holds only for a symmetrical wing not generating lift. A perhaps more plausible reason for why an airplane wing generates lift is because of Newton's third law which states "for every action there is an equal and opposite reaction". The airfoil changes the direction of the air. It sends a stream of air in the opposite direction to the lift, in order to send the wing upward. Following from existing steady

† 2006년 12월 19일 접수~2007년 2월 9일 게재승인
* Major, Korea Air Force Headquarter, KyeRyong, ChungNam
주저자 이메일 : young_sun_hong@yahoo.com

state aerodynamic theories, it has been claimed that insects and birds cannot fly because the existing theories used have considered mostly two dimensional effects to explain how animals generate lift. To make matters worse, insects and birds fly at low Reynolds numbers. The performance of low Reynolds number airfoils is entirely dictated by the relatively poor separation resistance of the laminar boundary layer. Therefore, much research has attempted to show that insects and birds use specific mechanisms or gaits to get more lift in low Reynolds number flight, such as clap and fling, delayed stall, vortex ring gait. Even if flat plate wings are flapped with zero chordwise pitch angle of attack and no relative wind, they have been shown to generate lift forces(positive and negative depending on the sense of the stroke assuming no feathering) due only to the flapping motion. However, most of research tried to show the average lift or thrust of flapping cycle in various flapping frequencies, wing planforms and stream velocities, not the instantaneous force variation of flapping motion from the beginning of the downstroke to the end of the upstroke[1,2]. Therefore, this research measured the instantaneous force variation of pure flapping cycle. Those result could effect to design MAV operated by flapping motion.

2. Experimental Approach

A flat plate wing with zero degrees chordwise pitch angle of attack cannot produce lift using conventional chordwise aerodynamics alone. However, in hover, with no forward relative velocity and zero degrees angle of attack, flapping flat plate wings produce lift. In the experiments performed for this paper, the flapping motion is considered pure(downstroke and upstroke). No changes in chordwise pitch angle are made.

The experimental procedure consisted of two primary components : Measurement of the lift force generated by the flapping mechanism through force transducer measurement(Interface SSM A5 250) and determination of the inertial force contribution to the total lift force generated through the use of a High speed camera (FASTCAM Ultima ADX 1000 frames per second).

A. Flapping Mechanism and Various Wings

The flapping mechanism was adapted from a Cybird P1 remote control ornithopter model. The flapping mechanism is powered by a DC power supply. Figure 1 shows the flapping mechanism used in the experiment and the operating angle of the flapping mechanism. The gear box that generates the flapping motion is attached rigidly at the leading edge, but not at the trailing edge, which means that the translational axis is only located in leading-edge.

Figure 2 and Table 1 show the various wings, which were used in the experiment. The flapping

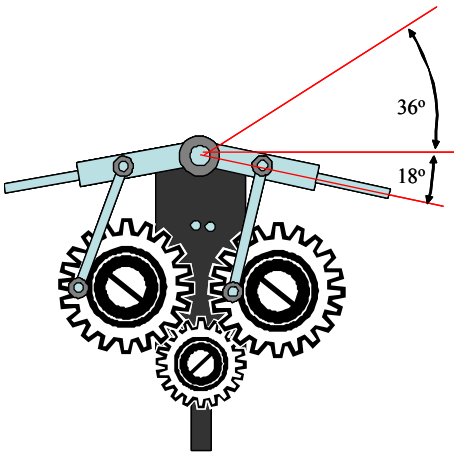

[Figure 1] The operating angle of the flapping mechanism

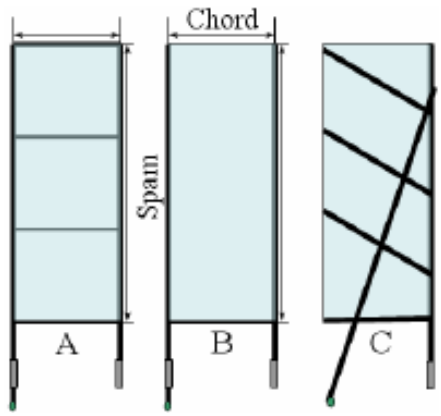

[Figure 2] Various wing shapes tested

[Table 1] Various wings used in the experiment

Wing #	Semi-Span (cm)	Chord (cm)	Aspect Ratio	Type	Mass	Flat or Cambered
1	20	10	4	A	15.99g	Flat
2	15	10	3	C	9.79g	Flat
3	15	7.5	4	C	7.78g	Flat
4	15.5	7.5	4.1	B	7.34g	Flat
5	5.5	7.5	1.5	B	3.48g	Flat
6	15.5	7.5	4.1	B	7.34g	Cambered*

* Curved 25 degrees at 5cm from the end of the wing

mechanism was set at various flapping frequencies using a high precision strobe.

B. Bending of the Wing

A limited number of theoretical studies addressing local bending moments in flapping wings suggest that inertial elastic forces may play a larger role than aerodynamic forces in determining instantaneous wing shape. For example, Ennos[3](1989) estimated that spanwise bending moments due to the inertia of flapping wings are at least twice as large as those due to aerodynamic forces, and showed that wing inertia

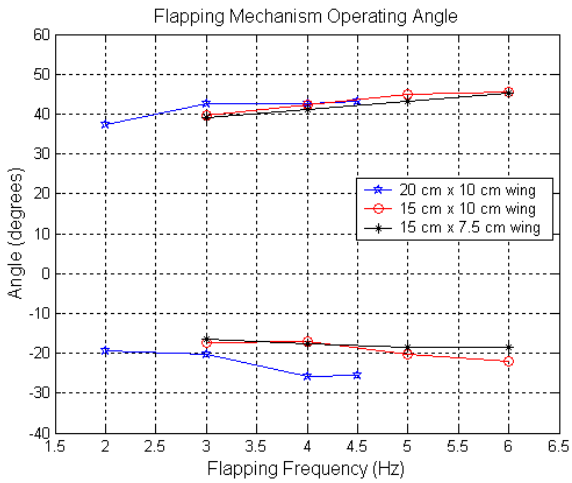

[Figure 3] The operating angles of the flapping mechanism as a function of flapping frequency

alone could cause the tip to base torsional wave seen in many insect wings during supination[4]. The operating angle of the flapping wing mechanism is a weak function of the wing length, the wing material and the flapping frequency. As an example, Figure 3 shows the flapping wing operating angle as a function of the flapping frequency. As the flapping frequency, wing mass and area increase, the operating angles of the flapping wings also increase. The flapping mechanism was designed to be operated at various flapping frequencies. The flapping mechanism without the wing was designed to be operated at the same operating angle. However, the operating angle of the flapping wing also varies due to inertial effects.

C. Input Power

The input D.C voltage required to flap these wings is shown in Figure 4. The input D.C. voltage is directly proportional to the flapping frequency[5]. The input D.C. voltage also depends upon the mass and area of the wing.

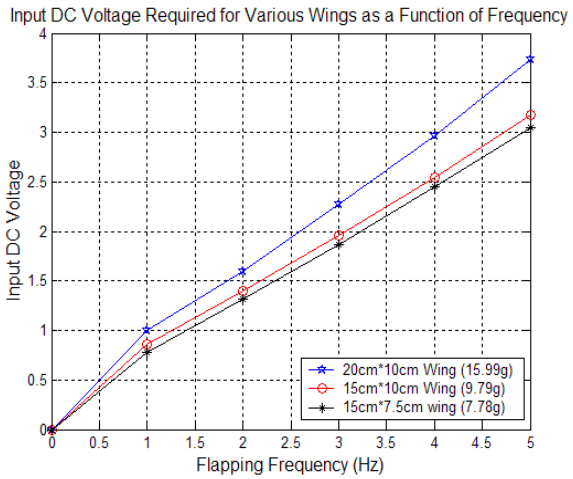

[Figure 4] The input D.C. Voltage required to flap the various wings as a function of flapping frequency. The input D.C. voltage to flap the #1, 2 and 3 wings from Table 1.

3. Total Lift Force

The flapping frequency and wing surface area are key parameters that have strong influence on force generation for flapping flight. Figure 5 presents the variation in lift force with flapping frequency for a 1 second time interval. A higher flapping frequency resulted in a larger lift force.

Figure 6 shows the total lift force variation with time for 3 of the wings tested. The total lift force which is shown in Figure 6 was averaged across 50 flapping cycles. The total lift force is influenced by the inertial contribution and the aerodynamic force. As seen in Figure 6, total lift force is related to the flapping frequency, wing mass and area of the wing. As the flapping frequency is increased, the difference in lift force is clearly seen : i.e. the larger the wing surface and the heavier the wing mass, the higher the lift force. However, maximum lift force of 20cm×

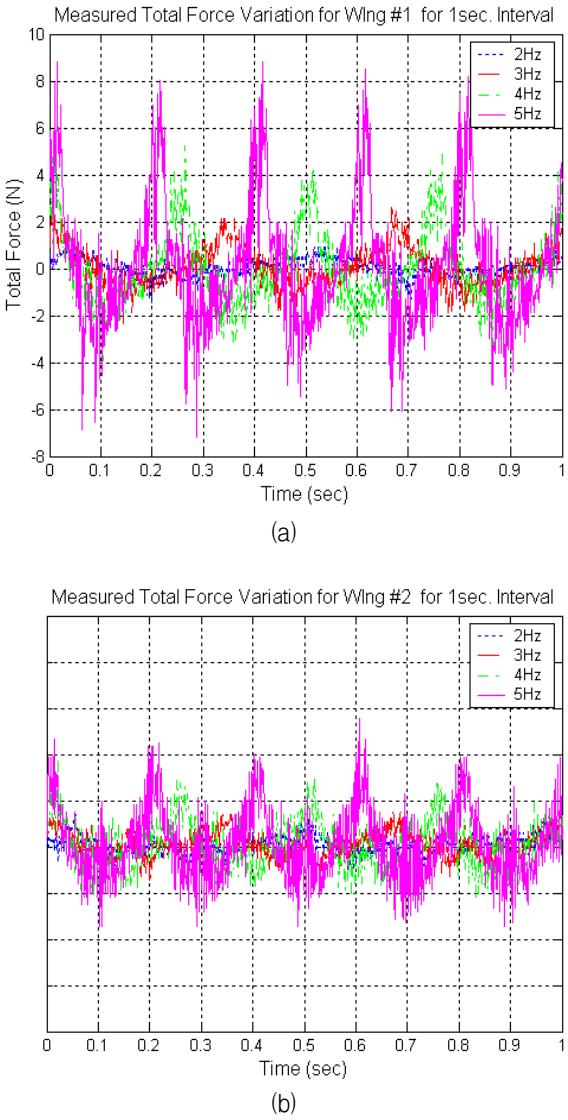

[Figure 5] Force variation of flapping wing with various flapping frequencies. (a) The lift force variation as a function of time for different flapping frequencies for the 20cm×10cm wing(#1 wing in Table 4.1) for a 1 second time interval. (b) The lift force variation as a function of time for different flapping frequencies for the 15cm×10cm wing(#2 wing in Table 4.1) for a 1 second time interval.

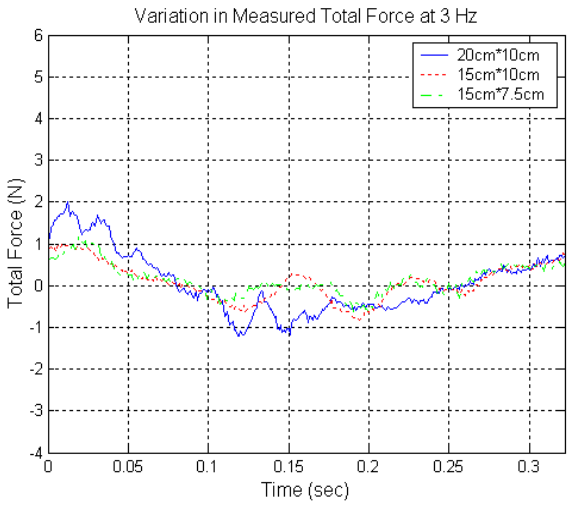

(a)

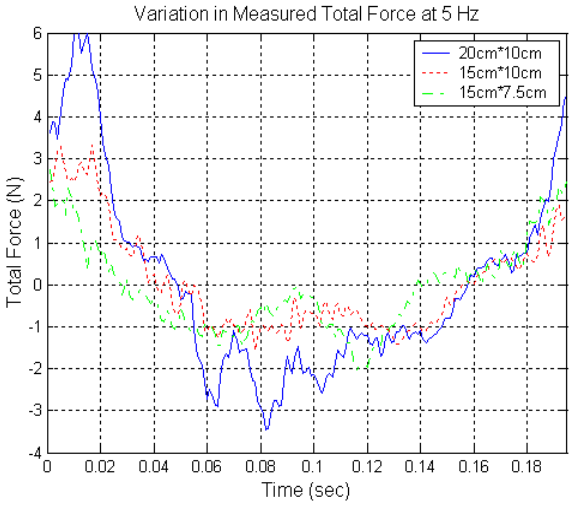

(b)

[Figure 6] Force variation of flapping wing with various flapping wings. (a) The variation in total lift force of various wings at a flapping frequency of 3Hz. (b) The variation in total lift force of various wings at a flapping frequency of 5Hz.

10cm wing during a flapping cycle is almost twice as much as that of 15cm×10cm in both frequencies(3Hz and 5Hz).

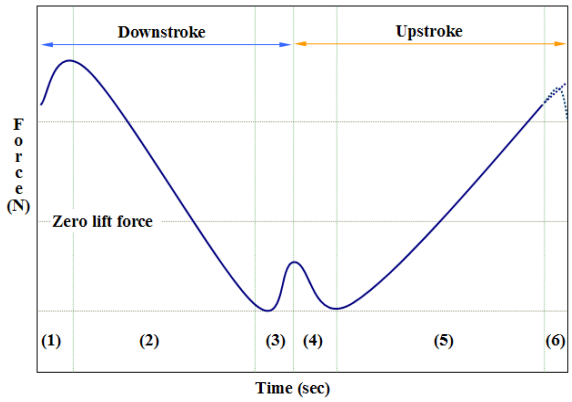

[Figure 7] The uniform trend of the total lift force variation during one cycle.

From Figure 6, the uniform trend of force variation during one cycle except for the 20cm× 10cm wing(#3 wing in Table 1) can be seen. Using the high frame rate camera(FASTCAM-Ultima APX 1000 frame/sec) we found that the 20cm×10cm wing experienced a 2^{nd} order oscillation incited by aeroelastic coupling in the thin wing during down and upstrokes, especially at the end and beginning of each stroke.

Figure 7 shows the uniform trend in force variation which is obtained using various wings and frequencies.

(1) At the beginning of the downstroke, the total lift force is a positive lift force. The total lift force increases until a certain point in the downstroke and peaks before the middle of the downstroke.
(2) The total lift force decreases to negative lift force until near the end of the downstroke. In the middle of the downstroke, the total lift force is less than zero.
(3) The flapping wings produce another small peak in force almost at the end of the downstroke.
(4) During the upstroke, a large lift force peak at

the beginning of the upstroke decreases until before the middle of the upstroke.

(5) The total lift force also increases up to the end of the upstroke.

(6) Near the end of the upstroke, the lift force decreases a little or increases continuously depending on the wing tested.

The total lift force in the downstroke is usually higher than that of the upstroke at the same angle in the flapping arc. The total lift force is the combination of forces due to the mass of the wing and acceleration and the aerodynamic force due to the flapping motion. Therefore, the total force *variation* is also influenced by the inertial force and the aerodynamic force.

4. Inertial and Aerodynamic Force

This total lift force will subsequently be divided up into the force due to the combination of the mass of wing and it's velocity as a function of time and the aerodynamic force due to the flapping motion[6~8]. Since the inertial force is a direct function of the mass of the wing, the total force is also related to the mass of the wing. In addition, it can be observed that the aerodynamic force is a function of the area and AR of the wing. Flapping wings produce forces as they accelerate and decelerate through a fluid. Aerodynamic forces are related to the fluid through which the wing moves. The flapping frequency is usually a key parameter in aerodynamic efficiency and has an effective influence on force generation in flapping flight. Lu[9](2003) obtained the experimental results which is the lift and drag coefficients for 0.5Hz and 2Hz flapping frequency at the same amplitudes. The results show that the lift coefficient at 2Hz is higher than that at 0.5Hz due to the inertial effect. On the other hand, inertial forces are also determined by the mass of the wing and its material properties. In insects, these forces bend and twist the wings during flight, resulting in passive shape changes that may affect many aspects of flight performance. Some estimates of overall wing inertia suggest that inertial forces are generally higher than aerodynamic forces[10~13], whereas other studies conclude the opposite[14,15]. It depends on the masses, areas or properties of the wing and mass distribution as well.

A. Inertial Force

One method of determining the inertial contributions in order to measure total force in flapping wings includes a vacuum container and a brass rod substituting for the uniform wing. An accelerometer can also measure the force due to the mass of wing at the mechanism's body center[16]. The inertial force produced by wing motion cannot accelerate the mechanism's center of mass. Sane[17](2001) used the blade element method to estimate the inertial forces and Singh[18](2005) developed theoretical methods to calculate the inertial force. In our case, a high frame rate camera(FASTCAM-Ultima APX, 1000 frame/sec) was used to take the images of the flapping mechanism/wing using a fixed frame rate (constant time interval between images).

The inertial force is defined as the force due to mass and acceleration of the flapping mechanism. Hence, it can be obtained using Newton's second law($F=m \cdot a$). Analyzing the images, angular velocity and angular acceleration can be obtained from these images. The forces in the x and y direction of the flapping mechanism are calculated using angular velocity and angular acceleration.

$$\omega = \frac{\Delta\theta}{\Delta t} \quad \text{(a)} \qquad \alpha = \frac{\Delta\omega}{\Delta t} \quad \text{(b)}$$
$$V_T = r\omega \quad \text{(c)} \qquad a_T = r\alpha \quad \text{(d)} \qquad (1)$$

where and a_T are tangential velocity and acceleration of wings.

Approximate values of flapping angles are required to generate the inertial force distribution from a set of experimentally V_T determined discrete points using a polynomial. To obtain the inertial force variation, the smoothed flapping angle distribution can be approximated with the polynomial in which following equations(Eq (2), (3)) have the minimum value or the closest value to 1, from a 2nd to 9th degree polynomial. Usually, the highest degree polynomial has the minimum value with the Least Square Interpolant.

1) Least Square Interpolant

$$E = \sum_{i=1}^{n} [y_i - \hat{y}]^2 \qquad (2)$$

2) The coefficient of determination

$$R^2 = \frac{\sum_{i=1}^{n} [\hat{y}_i - \bar{y}]^2}{\sum_{i=1}^{n} [y_i - \bar{y}]^2} \qquad (3)$$

Then, using F=m · a and (1), the inertial force in the y axis which is the axis aligned with lift and gravity force is obtained. Figure 8(a) shows the total lift force variation, the estimated total lift force variation and the inertial force variation throughout the entire cycle from the beginning of the downstroke to the end of upstroke(Wing #2 at 4Hz). Figure 8(b) shows the resulting lift force contribution of the aerodynamic force in which the inertial force is subtracted from the total lift force measured by the force transducer.

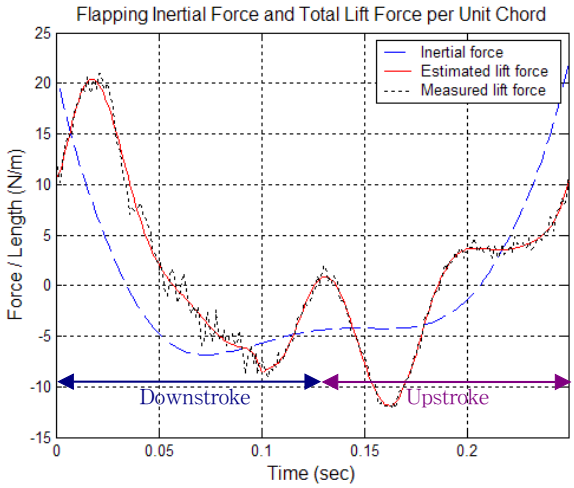

(a)

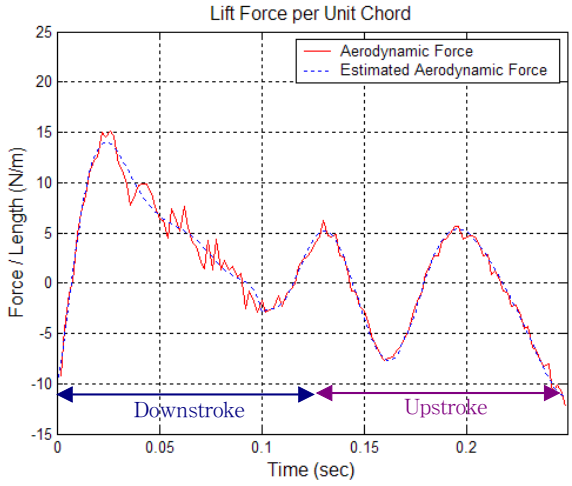

(b)

[Figure 8] The force variation of flapping wing during one entire cycle(Wing #2 at a flapping frequency of 5Hz). (a) The total force variation as measured by the force transducer(black dotted line), the polynomial curve fit approximation of the total force variation(red solid line), and the inertial force variation(blue dashed line) through one cycle from the beginning of the downstroke to the end of upstroke. (b) The polynomial curve fit approximation of the aerodynamic contribution to the lift force(dotted blue line) and the lift force (red solid line) resulting from the aerodynamic force.

As some estimates have mentioned[19~21], the inertial force is higher than the aerodynamic force for all cases using wing #1, 2 and 3 at 3Hz, 4Hz and 5Hz, 6Hz flapping motion. As the flapping frequency increases, inertial force and aerodynamic force are also increased. From the lift force variation due to the aerodynamic force, uniform trends during the entire cycle of the flapping motion are observed. Even though the wing size and flapping frequency have been changed, in the case without the circular vortex in the spanwise direction, the trends and shapes for the lift force resulting from the aerodynamic force are consistent. However, for the 20cm×10cm rectangular wing(Figure 6) the uniform trend was not observed when compared to 15cm×10cm and 15cm×7.5cm rectangular wings. It is suspected that this is due to nonlinear aeroelastic coupling during the downstroke and upstroke, especially at higher frequency.

B. Aerodynamic Force

The trends for temporal variation in aerodynamic lift force and measured total lift force have nearly identical shape. Figure 9 shows the trend for lift force variation due to the aerodynamic force. The

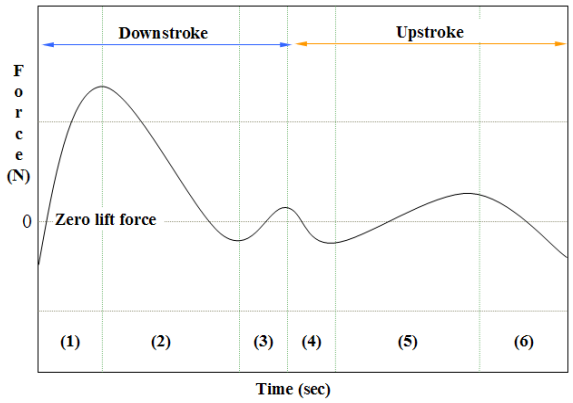

[Figure 9] The trend of for lift force variation due to aerodynamic force.

numbers denote specific sub phases in the flapping motion that will be described in detail in the next section.

In referring to Figure 10, the full cycle of the flapping motion will be divided into 6 sub phases for the purposes of evaluation of the transient forces using the DPIV results. In order to simplify the explanation later, the 6 sub phases will be introduced first.

1) The start of the downstroke : This phase begins from the starting point of the downstroke to the acceleration of the wing. Hence, acceleration is maximized in the downward direction. At the beginning of the downstroke, the inertial lift force is the greatest (+). Initially, the resulting aerodynamic force is reflected in negative lift force, most likely because the spanwise velocity over the bottom surface of the flapping wing is greater than the velocity over the top surface(Figure 10(a)).
2) The downstroke phase : The wing moves downward along the flap arc. The wing is accelerated while moving downward. It is also decelerated as it approaches the end of the downstroke. In the middle of the downstroke, the acceleration is zero. The inertial force decreases continuously until the point where the deceleration starts near the end of the downstroke. The aerodynamic force peaks at a specific point in the downstroke. The peak point is affected by the velocity distribution along the wing and the vortex effect(Figure 10 (b)).
3) The end of the downstroke : The wing is decelerated to change the direction of the flapping wing from downward to upward. As the deceleration progresses, the inertial lift force increases slightly. The aerodynamic force

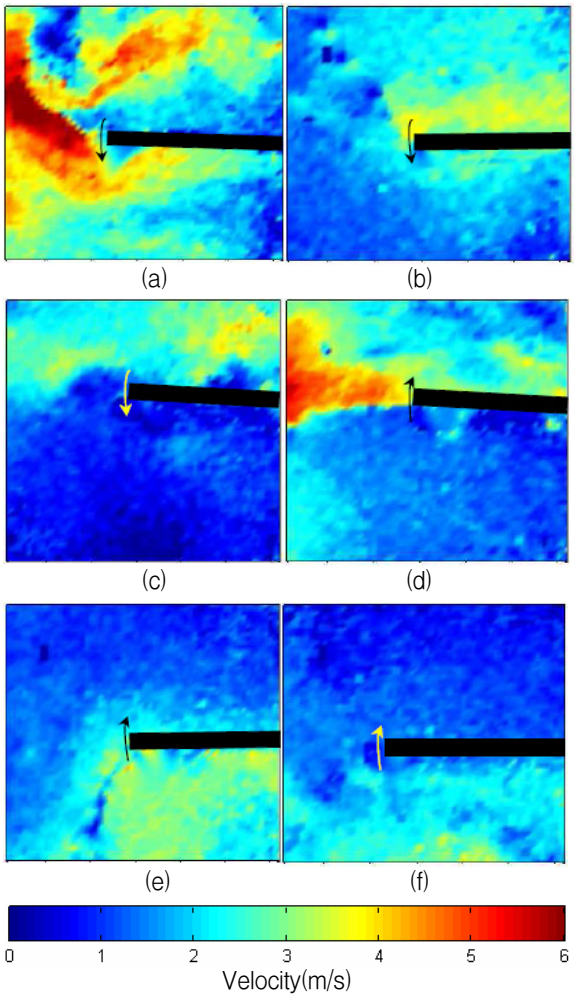

[Figure 10] PIV images at different locations in the flapping arc during the flapping motion. The flap angle of each position is as follows : (a) +39° (b) 1° (c) 16° (d) 17° (e) 1° (f) +38° (a) The initial stage of the stroke to downward. It is shown that there is a spanwise velocity difference between the upper and lower surfaces of the wing. The wing normally generates a negative lift force at this location in the flap arc. (b) During the downstroke, the wing can generate a positive lift force due to the velocity distribution across the lower and upper surfaces. (c), (d) Near the end of the downstroke and the start of the upstroke. The wing usually generates positive lift force. (e), (f) The stages including the upstroke. The flapping wing usually generates a negative lift force.

experiences a small peak almost at the end of the downstroke due to the velocity distribution along the wingspan(Figure 10 (c)).

4) The start of the upstroke : The wing is accelerated upward to begin moving upward. The acceleration is then maximized in the upward direction. The inertial force increases continuously until the end of the upstroke. The aerodynamic force creates a positive lift force, in spite of the upstroke, due to the velocity distribution across the wing(Figure 10 (d)).
5) The upstroke phase : The wing moves upward through the flapping arc. The wing is accelerated while moving upward. It is also decelerated as the wing approaches near the end of the upstroke. In the middle of the upstroke, the acceleration is zero. The aerodynamic force is usually negative lift force during the unfeathered upstroke. However, near the point that deceleration begins, as the velocity distribution along the wing changes, the aerodynamic force is positive lift for a while. The aerodynamic force achieves a small peak near just after the middle of the upstroke. The lift force decreases subsequently until the end of the upstroke(Figure 10 (e)).
6) The end of the upstroke : The wing decelerates to change the direction of the flapping wing from upward to downward. The velocity distribution along the wing in spanwise direction explains why it could generate negative lift force at the end of the upstroke (Figure 10 (f)).

The following instantaneous PIV images were taken of the wingtip with the stroke direction indicated for each sub phase.

5. Conclusion

A flat plate flapping wing without forward relative velocity and without change in pitch angle generates lift force. The experimental procedure consisted of two components : Measurement of the lift force generated by the flapping mechanism through force transducer measurement and determination of the inertial force contribution to the total lift force generated through the use of a high speed camera. Using a combination of force transducer measurement to quantify net lift force and high frame rate camera to quantify and subtract inertial contributions, the trends for temporal variation in measured total lift force (measured by the force transducer) and total aerodynamic lift force(inertial force is subtracted from the total lift force) have nearly identical shape for various flapping frequencies and various wing planform sizes. The aerodynamic force positively peaks at a specific point in the downstroke and the end of the downstroke. The aerodynamic force is positive lift for a while during the upstroke. Total lift force is related to the flapping frequency, wing mass and area of the wing. Therefore, the result of this research can effect to design optimized flapping mechanism and wings, especially operating angle of flapping wing.

Reference

[1] Pornsin-Sisirak T., Tai Y. C., et al, "Microbat- A Palm-Sized Electrically Powered Ornithopter", 2001 NASA/JPL Workshop On Biomorphic Robotics, Pasadena, CA, Aug 2000.

[2] Che-Shu, Lin, Chyanbin, Hwu, Wen-Bin, Young, "The Thrust and Lift of an Ornithopter's Membrane Wings with Simple FLapping Motion", Aerospace Science and Technology 10, 111～119, 2006.

[3] Ennos, A. R., "Inertial And Aerodynamic Torques On The Wings Of Diptera In Flight", Journal Of Experimental Biology, Vol. 142, pp.87～95, 1989.

[4] Ennos, A. R., "The Inertial Cause Of Wing Rotation In Diptera", Journal Of Experimental Biology, Vol. 140, pp.161～169, 1988.

[5] Pornsin Sisirak T., Tai Y. C., et al, "Microbat A Palm Sized Electrically Powered Ornithopter", 2001 NASA/JPL Workshop On Biomorphic Robotics, Pasadena, CA, Aug 2000.

[6] Sane S. P. And Dickinson M. H., "The Aerodynamic Effects Of Wing Rotation And A Revised Quasi Steady Model Of Flapping Flight", The Journal Of Experimental Biology, Vol. 205, pp.1087～1096, 2002.

[7] Combes, S. A. And Daniel, T. L., "Into Thin Air : Contributions Of Aerodynamic And Inertial Elastic Forces To Wing Bending In The Hawkmoth Maduca Sexta", Journal Of Experimental Biology, Vol. 206, pp.2999～3006, 2003.

[8] Maybury, Will J. And Lehmann, Fritz Olaf, "The Fluid Dynamics Of Flight Control By Kinematic Phase Lag Variation Between Two Robotic Insect Wings", Journal Of Experimental Biology, Vol. 207, pp.4707～4726, 2004.

[9] Lu X. Y., Yang J. M. And Yin X. Z., "Propulsive Performance And Vortex Shedding Of A Foil In Flapping Flight", Acta Mechanica, Vol. 165, pp.189～206, 2003.

[10] Ellington, C. P., "The Aerodynamics Of Insect Flight. II. Morphological Parameters", Philosophical Transactions Of The Royal Society Of London. Series B, Biological Sciences, Vol. 305, pp.17～40 1984.

[11] Lehmann, F. O. And Dickinson, M. H., "The Changes In Power Requirements And Muscle Efficiency During Elevated Force Production In The Fruit Fly Drosophila Melanogaster", Journal Of Experimental Biology, Vol. 200, pp.1133~1143, 1997.

[12] Wilkin, P. J. And Williams, M. H, "Comparison Of The Aerodynamic Forces On A Flying Sphingid Moth With Those Predicted By Quasi Steady Theory", Physiological Zoology, Vol. 66, pp.1015~1044, 1993.

[13] Zanker, J. M. And Gotz, K. G., "The Wing Beat Of Drosophila Melanogaster. II. Dynamics", Phiosophical Transaction Of Royal Society Of London. B, Vol. 327, pp.19~44, 1990.

[14] Sun, M. And Tang, J. "Lift And Power Requirements Of Hovering Flight In Drosophila Virilis", Journal Of Experimental Biology, Vol. 205, pp.2413~2427, 2002.

[15] Wakeling, J. M. And Ellington, C. P, "Dragonfly Flight. III. Lift And Power Requirements", Journal Of Experimental Biology, Vol. 200, pp.583~600, 1997.

[16] Bilo, Dietrich, et al, "Measurement Of Linear Body Accelerations And Calculation Of The Instantaneous Aerodynamic Lift And Thrust In A Pigeon Flying In A Wind Tunnel", Biona Report 3. Stuttgart, Gustav Fischer, 1985.

[17] Sane, S. P. And Dickinson, M. H., "The Control Of Flight Force By A Flapping Wing : Lift And Drag Production", The Journal Of Experimental Biology, Vol. 204, pp.2607~2626, 2001.

[18] Singh, B., Ramasamy, M., Chopra, I. And Leishman, J. G., "Insect Based Flapping Wings For Micro Hovering Air Vehicles : Experimental Investigations", American Helicopter Society International Specialists Meeting On Unmanned Rotorcraft, Phoenix, AZ, Jan 2005.

[19] Lehmann, F. O. And Dickinson, M. H., "The Changes In Power Requirements And Muscle Efficiency During Elevated Force Production In The Fruit Fly Drosophila Melanogaster", Journal Of Experimental Biology, Vol. 200, pp.1133~1143, 1997.

[20] Wilkin, P. J. And Williams, M. H., "Comparison Of The Aerodynamic Forces On A Flying Sphingid Moth With Those Predicted By Quasi Steady Theory", Physiological Zoology, Vol. 66, pp.1015~1044, 1993.

[21] Zanker, J. M. And Gotz, K. G., "The Wing Beat Of Drosophila Melanogaster. II. Dynamics", Phiosophical Transaction Of Royal Society Of London. B, Vol. 327, pp.19, 1990.